THE JOURNAL OF BIOLOGICAL CHEMISTRY VOL. 291, NO. 36, pp. 18843–18852, September 2, 2016

Mice Deficient in Angiopoietin-like Protein 2 (*Angptl2*) Gene Show Increased Susceptibility to Bacterial Infection Due to Attenuated Macrophage Activity*

Received for publication, February 9, 2016, and in revised form, June 30, 2016 Published, JBC Papers in Press, July 11, 2016, DOI 10.1074/jbc.M116.720870

Masaki Yugami[‡§1], Haruki Odagiri[‡§1], Motoyoshi Endo[‡2], Hiroyasu Tsutsuki[¶], Shigemoto Fujii[‖], Tsuyoshi Kadomatsu[‡], Tetsuro Masuda[‡§], Keishi Miyata[‡], Kazutoyo Terada[‡], Hironori Tanoue[‡§], Hitoshi Ito[‡§], Jun Morinaga[‡], Haruki Horiguchi[‡], Taichi Sugizaki[‡], Takaaki Akaike[‖], Tomomi Gotoh[‡], Toshiyuki Takai[**], Tomohiro Sawa[¶], Hiroshi Mizuta[§], and Yuichi Oike[‡ ‡‡3]

From the Departments of [‡]Molecular Genetics, [§]Orthopedic Surgery, and [¶]Microbiology, Graduate School of Medical Sciences, Kumamoto University, Kumamoto 860-8556, Japan, [‖]Department of Environmental Health Sciences and Molecular Toxicology, Tohoku University Graduate School of Medicine, Sendai 980-8575, Japan, [**]Department of Experimental Immunology, Institute of Development, Aging and Cancer, Tohoku University, Sendai 980-8575, Japan, and [‡‡]Core Research for Evolutional Science and Technology (CREST), Japan Agency for Medical Research and Development (AMED), Tokyo 102-0076, Japan

Macrophages play crucial roles in combatting infectious disease by promoting inflammation and phagocytosis. Angiopoietin-like protein 2 (ANGPTL2) is a secreted factor that induces tissue inflammation by attracting and activating macrophages to produce inflammatory cytokines in chronic inflammation-associated diseases such as obesity-associated metabolic syndrome, atherosclerosis, and rheumatoid arthritis. Here, we asked whether and how ANGPTL2 activates macrophages in the innate immune response. ANGPTL2 was predominantly expressed in proinflammatory mouse bone marrow-derived differentiated macrophages (GM-BMMs) following GM-CSF treatment relative to anti-inflammatory cells (M-BMMs) established by M-CSF treatment. Expression of the proinflammatory markers IL-1β, IL-12p35, and IL-12p40 significantly decreased in GM-BMMs from *Angptl2*-deficient compared with wild-type (WT) mice, suggestive of attenuated proinflammatory activity. We also report that ANGPTL2 inflammatory signaling is transduced through integrin $\alpha5\beta1$ rather than through paired immunoglobulin-like receptor B. Interestingly, *Angptl2*-deficient mice were more susceptible to infection with *Salmonella enterica* serovar Typhimurium than were WT mice. Moreover, nitric oxide (NO) production by *Angptl2*-deficient GM-BMMs was significantly lower than in WT GM-BMMs. Collectively, our findings suggest that macrophage-derived ANGPTL2 promotes an innate immune response in those cells by enhancing proinflammatory activity and NO production required to fight infection.

The mammalian immune system is critical to combat infectious pathogens and comprises two branches, the innate and acquired immune systems (1). Unlike the acquired system, innate immunity is activated to provide an immediate response to pathogens (2). Thus, it constitutes the first line of host defense against pathogens and is mediated by phagocytes such as macrophages. In addition, development of inflammation is important for host resistance to infection (1), and proinflammatory macrophages are crucial to support resistance to intracellular bacteria and control the acute phase of infection (3–10).

We reported previously that ANGPTL2[4] signaling functions in tissue repair through adaptive inflammation and angiogenesis (11, 12), whereas excess ANGPTL2 signaling causes chronic maladaptive inflammation and subsequent pathological irreversible tissue remodeling, leading to the development of various diseases such as obesity-associated metabolic disease, atherosclerotic vascular disease, rheumatoid arthritis, and some cancers (11, 13–15). In these pathologies, ANGPTL2 activates macrophages, which participate in disease progression, suggesting that ANGPTL2 promotes proinflammatory phenotypes and stimulates inflammatory cytokine secretion by macrophages. Although these activities are associated with disease, inflammation is required for the innate immune system to fight infection.

In this study, we asked whether and how ANGPTL2 functions in the innate immune response. We found that ANGPTL2 is predominantly expressed in proinflammatory bone marrow-derived differentiated macrophages (GM-BMMs) established by treatment of mouse bone marrow cells with GM-CSF, and

* This work was supported by the Scientific Research Fund of the Ministry of Education, Culture, Sports, Science and Technology of Japan (Grants 15K20008, 25461192, and 15H01159), the Core Research for Evolutional Science and Technology (CREST) program of the Japan Science and Technology Agency (Grant 13417915), and the CREST program of the Japan Agency for Medical Research and Development (Grant 15gm0610007h0003). The authors declare that they have no conflicts of interest with the contents of this article.

[1] Both authors contributed equally to this work.
[2] To whom correspondence may be addressed: Dept. of Molecular Genetics, Kumamoto University, 1-1-1 Honjo, Kumamoto 860-8556, Japan. Tel.: 81-96-373-5142; Fax: 81-96-373-5145; E-mail: enmoto@gpo.kumamoto-u.ac.jp.
[3] To whom correspondence may be addressed: Dept. of Molecular Genetics, Kumamoto University, 1-1-1 Honjo, Kumamoto 860-8556, Japan. Tel.: 81-96-373-5140; Fax: 81-96-373-5145; E-mail: oike@gpo.kumamoto-u.ac.jp.

[4] The abbreviations used are: ANGPTL2, angiopoietin-like protein 2; BMM, bone marrow-derived differentiated macrophage; PIR-B, paired immunoglobulin-like receptor B; rANGPTL2, recombinant mouse ANGPTL2 protein; m.o.i., multiplicity of infection; TLR4, toll-like receptor 4; APC, allophycocyanin.

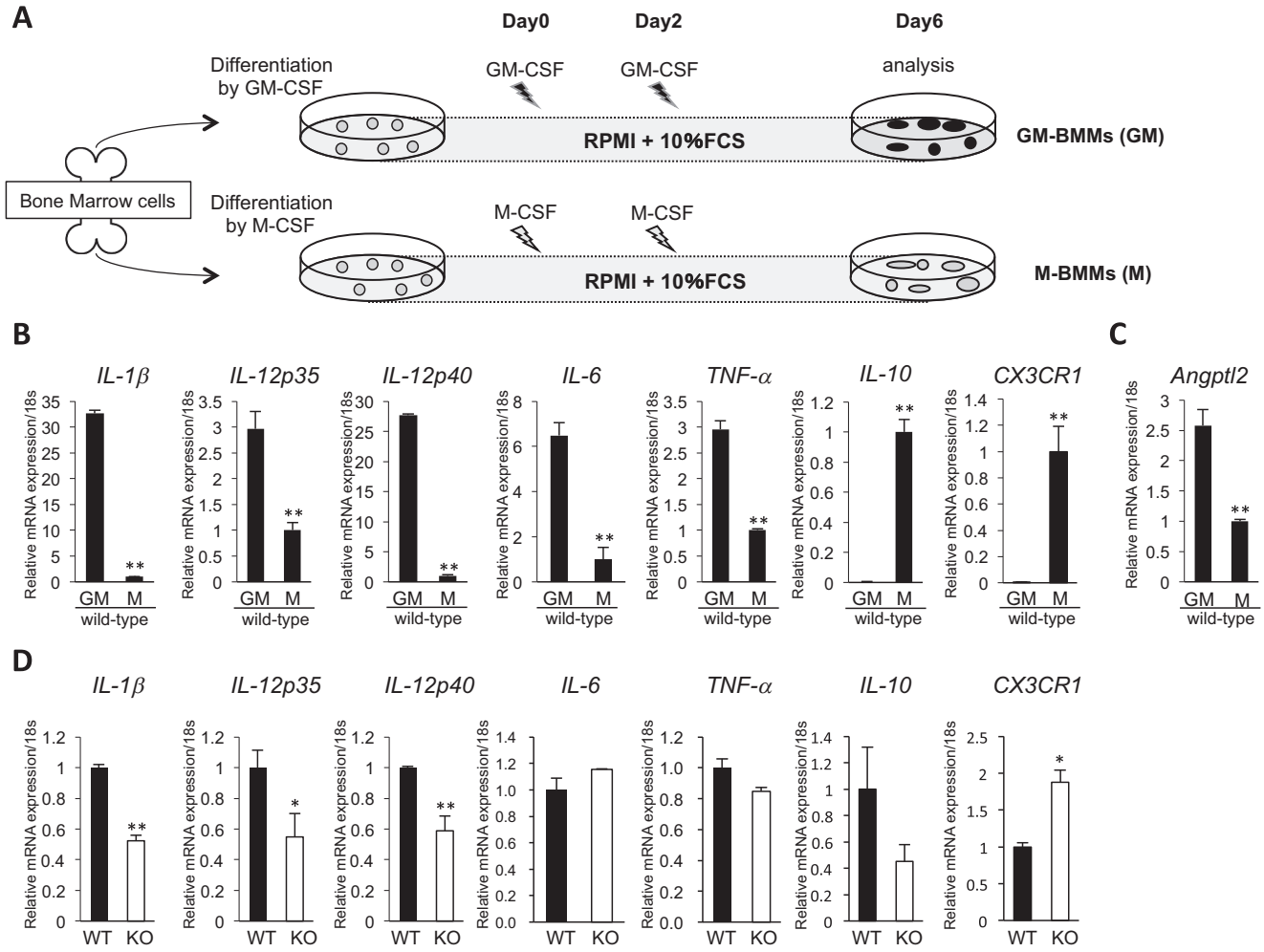

FIGURE 1. **Analysis of pro- and anti-inflammatory markers in GM-BMMs and M-BMMs.** *A*, differentiation protocols used to generate macrophages from bone marrow cells. *B*, relative expression of mRNAs encoding cytokines, chemokines, and chemokine receptors in GM-BMMs (*GM*) and M-BMMs (*M*) from WT mice ($n = 4$). Levels in M-BMMs were set at 1. *C*, relative *Angptl2* expression in GM-BMMs and M-BMMs from WT mice based on RT-PCR analysis ($n = 4$). Levels in M-BMMs were set at 1. *D*, relative expression of mRNAs encoding cytokines, chemokines, and chemokine receptors in GM-BMMs from WT and *Angptl2* KO mice ($n = 4$). Levels in WT were set at 1. *, $p < 0.05$; **, $p < 0.01$. Data are expressed as means ± S.E. (*error bars*) from three different experiments.

proinflammatory activity was attenuated in *Angptl2*-deficient relative to wild-type (WT) macrophages. In addition, we showed that ANGPTL2 activates macrophages through integrin $\alpha5\beta1$ rather than paired immunoglobulin-like receptor B (PIR-B). Interestingly, *Angptl2*-deficient mice were more susceptible to *Salmonella enterica* serovar Typhimurium infection than were WT mice. Moreover, nitric oxide (NO) production and phagocytosis ability by *Angptl2*-deficient GM-BMMs were significantly lower than in WT controls. These findings suggest that macrophage-derived ANGPTL2 stimulates innate immune defense capacity in macrophages by enhancing proinflammatory activity and NO production against infection.

Results

ANGPTL2 Treatment Promotes Proinflammatory Phenotypes in Macrophages in Vitro—To determine whether ANGPTL2 stimulates differentiation of pro- or anti-inflammatory macrophages, we undertook two *in vitro* tests of differentiation (Fig. 1*A*). In the first, we incubated bone marrow cells from wild-type adult mice with M-CSF to induce differentiated macrophages (M-BMMs), which exhibit anti-inflammatory phenotypes (16); in the other, we incubated bone marrow cells with GM-CSF to induce proinflammatory GM-BMMs (17, 18) (Fig. 1*A*). We then assessed expression of pro- or anti-inflammatory markers in both groups by quantitative real time PCR analysis (Fig. 1*B*). Relative levels of transcripts encoding proinflammatory markers such as IL-1β, IL-12p35, IL-12p40, IL-6, and TNF-α were significantly increased in GM-BMMs compared with M-BMMs, whereas transcripts encoding anti-inflammatory markers such as IL-10 and the chemokine receptor CX3CR1 were significantly up-regulated in M-BMMs compared with GM-BMMs (Fig. 1*B*) as anticipated. Next, we examined endogenous ANGPTL2 expression in these cells and found that GM-BMMs expressed higher ANGPTL2 levels than did M-BMMs, suggesting that ANGPTL2 expression is associated with proinflammatory activity (Fig. 1*C*).

Next, we compared gene expression profiles in GM-BMMs from WT *versus Angptl2* KO mice. Transcripts encoding proinflammatory markers such as IL-1β, IL-12p35, and IL-12p40, but not IL-6 and TNF-α, were significantly decreased, whereas transcripts encoding the anti-inflammatory marker CX3CR1, but not IL-10, were significantly up-regulated in GM-BMMs

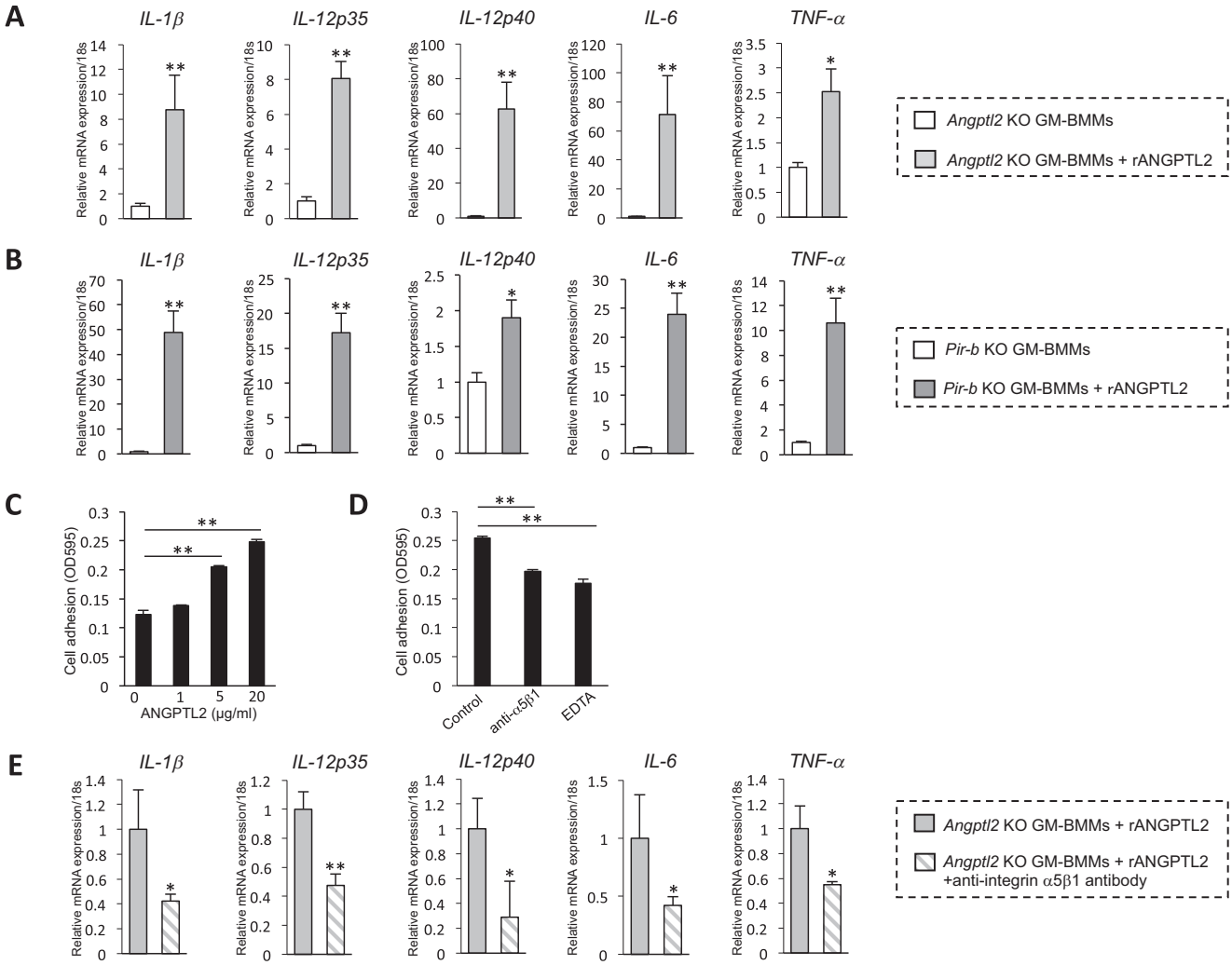

FIGURE 2. **Integrin $\alpha5\beta1$ partially mediates ANGPTL2-dependent proinflammatory phenotypes in macrophages.** *A*, relative expression of mRNAs encoding proinflammatory markers in cultured GM-BMMs from *Angptl2* KO mice incubated with or without rANGPTL2 ($n = 4$). Levels in untreated cells were set at 1. *B*, relative expression of transcripts encoding proinflammatory markers in cultured GM-BMMs from *Pir-b* KO mice incubated with or without rANGPTL2 ($n = 4$). Levels in untreated cells were set at 1. *C*, adhesion of GM-BMMs from WT mice to culture dishes coated with various concentrations of rANGPTL2 ($n = 4$). *D*, adhesion of GM-BMMs with rANGPTL2 (20 μg/ml) from WT mice preincubated with or without 25 μg/ml $\alpha5\beta1$ antibody ($n = 4$). As a negative control, adhesion was assayed in the presence of 10 mM EDTA, which inhibits integrin binding. *E*, relative expression of transcripts encoding proinflammatory markers in cultured GM-BMMs from *Pir-b* KO mice treated with rANGPTL2 with or without anti-integrin $\alpha5\beta1$ antibody ($n = 4$). Levels in GM-BMMs not treated with antibody were set at 1. *, $p < 0.05$; **, $p < 0.01$. Data are expressed as means ± S.E. (*error bars*) from two different experiments.

from *Angptl2* KO (Fig. 1*D*) compared with WT mice. These findings suggest that ANGPTL2 secretion by macrophages promotes proinflammatory phenotypes seen in those cells *in vitro*.

Integrin α5β1 Functions in Proinflammatory ANGPTL2 Signaling in GM-BMMs—To further assess ANGPTL2 signaling in inflammation, we conducted experiments supplementing cell cultures with recombinant mouse ANGPTL2 protein (rANGPTL2) and found that *Angptl2* KO GM-BMMs treated with rANGPTL2 showed up-regulated expression of proinflammatory markers, including IL-6 and TNF-α (Fig. 2*A*). Next, we asked what receptor might function in promoting proinflammatory phenotypes in GM-BMMs. The immune inhibitory human leukocyte immunoglobulin-like receptor B2, which contributes to hematopoietic stem cell stemness and leukemia development, reportedly functions as an ANGPTL2 receptor (19). PIR-B, its mouse orthologue (35), is reportedly expressed on and functions in immune cells (20), and *Pir-b* KO mice show heightened susceptibility to *Salmonella* infection (21). To determine whether PIR-B functioned as an ANGPTL2 receptor in promoting proinflammatory phenotypes in macrophages, we asked whether rANGPTL2 treatment could activate GM-BMMs established from *Pir-b* KO mice. rANGPTL2 treatment increased induction of proinflammatory transcripts such as IL-1β, IL-12p35, IL-12p40, IL-6, and TNF-α in GM-BMMs from *Pir-b* KO mice relative to untreated *Pir-b* KO controls (Fig. 2*B*), suggesting that in this context PIR-B does not mediate ANGPTL2-dependent proinflammatory signaling.

We reported previously that integrin $\alpha5\beta1$ functions as an ANGPTL2 receptor and that ANGPTL2 promotes inflammation through $\alpha5\beta1$/NF-κB signaling (11). Thus, here we asked whether ANGPTL2 binds integrin $\alpha5\beta1$ expressed on GM-BMMs prepared from wild-type mice. GM-BMMs adhered to mouse rANGPTL2-coated plates dose-dependently (Fig. 2*C*), binding that was inhibited by $\alpha5\beta1$-neutralizing anti-

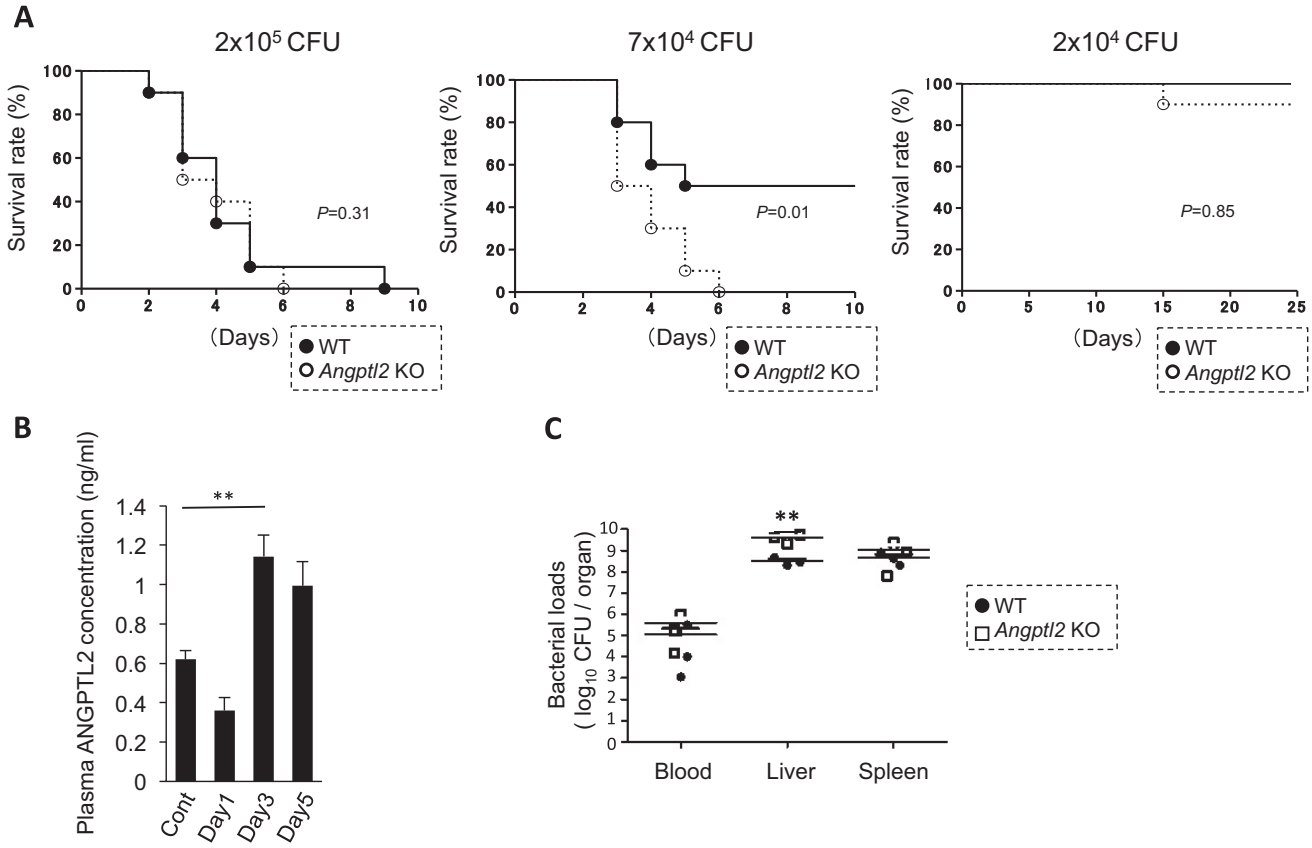

FIGURE 3. **Survival of WT or *Angptl2* KO mice following *Salmonella* infection.** *A*, WT (●) and *Angptl2* KO (○) mice ($n = 10$) were intraperitoneally injected with the indicated LT2 doses ($p = 0.31$, $p = 0.01$, $p = 0.85$, respectively, by log rank test). *B*, ANGPTL2 concentration at various days postinfection in plasma of WT mice intraperitoneally injected with 7×10^4 cfu of LT2. *C*, WT (●) and *Angptl2* KO (□) mice were intraperitoneally injected with 7×10^4 cfu of LT2. $\log_{10}$ values of LT2 cfu per organ represent individual mice ($n = 3$) at day 3. **, $p < 0.01$. Data are expressed as means ± S.E. (*error bars*) from one experiment. *Cont*, control.

body (Fig. 2*D*). Next, we asked whether treatment of GM-BMMs with that antibody would block proinflammatory signaling induced by ANGPTL2. We observed that treatment of GM-BMMs with integrin $\alpha5\beta1$ antibody partially inhibited induction of transcripts encoding the proinflammatory markers IL-1β, IL-12p35, IL-12p40, IL-6, and TNF-α by ANGPTL2 (Fig. 2*E*), suggesting that integrin $\alpha5\beta1$ functions in the macrophage response to ANGPTL2.

Angptl2 KO Mice Are More Susceptible to Salmonella Infection than Are WT Mice—Proinflammatory macrophages mediate resistance to intracellular pathogens (22–24). To evaluate ANGPTL2 function in proinflammatory macrophages, we generated *in vivo* models of WT or *Angptl2* KO mice infected with the *Salmonella enterica* serovar Typhimurium LT2, a Gram-negative, facultative intracellular pathogen that grows outside and inside of host cells. Mutant and WT mice were intraperitoneally infected with various LT2 doses (from 2×10^4 to 2×10^5 colony-forming units (cfu)/mouse) in groups of 10 per dose, and their survival was monitored for 4 weeks thereafter. In both groups, mice inoculated with high doses (2×10^5 cfu/mouse) died within 9 days of infection (Fig. 3*A*, *left panel*). At middle doses (7×10^4 cfu/mouse; Fig. 3*A*, *middle panel*), differences in survival were more apparent: many infected *Angptl2* KO mice showed signs of morbidity sooner than did WT mice during the course of infection, and all *Angptl2* KO mice died by 6 days after infection. By contrast, only half of the WT mice died during the same period (Fig. 3*A*, *middle panel*). Plasma ANGPTL2 levels in LT2-infected WT mice were significantly increased by day 3 of infection (Fig. 3*B*). At low doses (2×10^4 cfu/mouse), all mice of either genotype survived except one *Angptl2* KO mouse (Fig. 3*A*, *right panel*). Next, to determine tissue localization of inoculated bacteria, we sacrificed mice receiving the midlevel dose (7×10^4 cfu/mouse) 3 days after infection and analyzed bacterial loads in organs such as blood, liver, and spleen. *Angptl2* KO mice showed higher bacterial loads in liver than did WT mice (Fig. 3*C*), suggesting that lowered immune defense seen in *Angptl2* KO mice may be associated with impaired bacterial replication.

Angptl2 KO GM-BMMs Show Impaired NO Production—Next, we measured NO production by GM-BMMs, an activity required for antibacterial responses (25–28). In these experiments, we estimated NO production by assaying for nitrite, a stable metabolite of NO (29, 30). GM-BMMs from *Angptl2* KO mice showed less nitrite production than did WT GM-BMMs at 6 and 12 h following exposure to LT2 at a multiplicity of infection (m.o.i.) of 1 (Fig. 4, *A* and *B*), supporting the idea that ANGPTL2 modulates bacterial clearance capacity through NO production. However, based on nitrite analysis, the difference in NO production by GM-BMMs in WT *versus Angptl2* KO mice was lesser at 12 h than at 6 h (Fig. 4, *A* and *B*), suggesting that bacterial clearance by macrophages is more impaired at early phases of infection in *Angptl2* KO relative to WT mice.

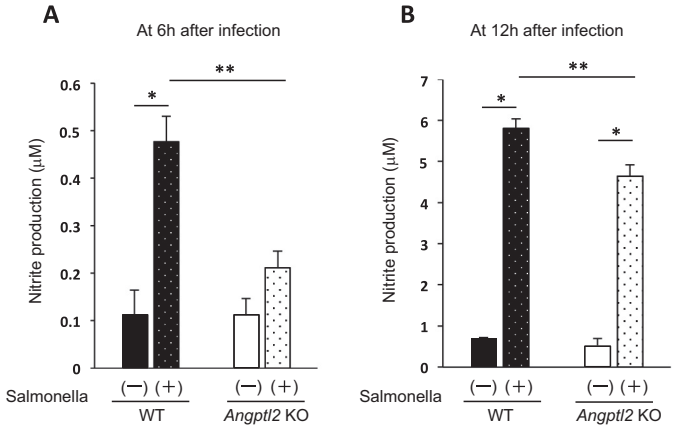

FIGURE 4. **NO production by GM-BMMs from WT and *Angptl2* KO mice infected with live LT2.** Shown is NO production by GM-BMMs from WT and *Angptl2* KO mice infected with live LT2 at an m.o.i. of 1 at 6 (*A*) or 12 (*B*) h after infection with live LT2 based on levels of the NO metabolite nitrite ($n = 4$). *, $p < 0.05$; **, $p < 0.01$. Data are expressed as means ± S.E. (*error bars*) from two different experiments.

Angptl2 KO GM-BMMs Show Impaired Bacterial Phagocytosis When Infection Level Is High—To assess phagocytic activity, we evaluated responses of GM-BMMs from WT or *Angptl2* KO mice to *in vitro* LT2 infection. At an m.o.i. of 1, we observed comparable phagocytosis in GM-BMMs of both genotypes (Fig. 5*A*). However, phagocytotic activity of GM-BMMs from *Angptl2* KO mice decreased relative to that in WT mice at higher m.o.i. values (>10) (Fig. 5*A*), suggesting that ANGPTL2 functions to control *Salmonella* infection by modulating phagocytosis. Therefore, we next examined expression of receptors that function in phagocytosis, namely the toll-like receptor 4 (TLR4) (CD284), Fc-γ receptor (CD16/32), scavenger receptor (CD36), and complement receptor (CD21/35), in GM-BMMs from WT or *Angptl2* KO mice. We observed no differences in expression of these receptors in GM-BMMs from mice of either genotype (Fig. 5*B*). Furthermore, when we assayed phagocytotic activity of GM-BMMs from WT or *Angptl2* KO mice using fluorescent beads, we observed no differences in GM-BMMs from WT or *Angptl2* KO mice (Fig. 5*C*). We conclude that potential changes in expression of major receptors associated with phagocytosis cannot account for impaired bacterial clearance seen in *Angptl2* KO GM-BMMs.

Angptl2 KO Peritoneal Macrophages Show Impaired Migration and NO Production—The studies above address activities in GM-BMMs derived from WT or *Angptl2* KO mice. Next, we assessed responses of primary peritoneal macrophages derived from WT and *Angptl2* KO mice. In unstimulated conditions, the number of peritoneal macrophages was comparable in mice of both genotypes (Fig. 6*A*). However, following thioglycollate stimulation, the number of peritoneal macrophages was significantly lower in *Angptl2* KO relative to WT mice (Fig. 6*B*). We then evaluated responses of peritoneal macrophages to *in vitro* LT2 infection. As observed in GM-BMMs (Fig. 5), we observed comparable phagocytosis in peritoneal macrophages of both genotypes at an m.o.i. of 1 (Fig. 6*C*). We also examined nitrite production in response to LT2 infection in peritoneal macrophages derived from mice of both genotypes and found that nitrite production by peritoneal macrophages from *Angptl2* KO mice was decreased relative to that seen in WT mice similar to our observations in GM-BMMs (Fig. 6*D*). Next, we compared gene expression profiles in peritoneal macrophages following lipopolysaccharide (LPS) treatment. Expression of the proinflammatory markers IL-1β and IL-12p40 was significantly lower in peritoneal macrophages from *Angptl2* KO mice (Fig. 6*E*). We also observed relatively lower TLR4 expression in peritoneal macrophages from *Angptl2* KO mice (Fig. 6*F*), suggesting that decreased TLR4 expression may underlie attenuation of macrophage activity seen in *Angptl2* KO mice.

Discussion

ANGPTL2 is a proinflammatory mediator that induces inflammation-associated diseases such as obesity-associated metabolic disease, atherosclerotic vascular disease, and rheumatoid arthritis (11, 13–15). Its role in infection, however, had not previously been addressed. Here, we focused on the function of macrophage-derived ANGPTL2 in infectious disease as macrophages are key inflammatory cells in this context. We found that ANGPTL2 was predominantly expressed in macrophages with proinflammatory phenotypes, and macrophage-derived ANGPTL2 likely activated other macrophages to acquire an inflammatory phenotype. *Angptl2* KO mice were also more susceptible to infection.

Our analysis shows that GM-BMMs, which exhibit proinflammatory macrophage phenotypes, express higher levels of ANGPTL2 than do anti-inflammatory M-BMMs. We also found that exogenous rANGPTL2 can rescue expression of mRNAs encoding inflammatory cytokines, including IL-1β, IL-12p35, IL-12p40, IL-6, and TNF-α, in *Angptl2* KO GM-BMMs, suggesting that the macrophage-derived ANGPTL2 mediates proinflammatory phenotypes in an autocrine manner. Conversely, levels of mRNAs encoding IL-6 and TNF-α were comparable in *Angptl2* KO and WT GM-BMMs in the absence of exogenous rANGPTL2. Thus, other mechanisms may regulate IL-6 and TNF-α expression in *Angptl2* KO GM-BMMs.

We reported previously that integrin α5β1 is an ANGPTL2 receptor and functions in inflammatory signaling (31), whereas others have reported that PIR-B, the mouse orthologue of human leukocyte immunoglobulin-like receptor B2, also acts as an ANGPTL2 receptor (19, 32). *Pir-b* KO mice are susceptible to *Salmonella* infection (21), raising the possibility that *Angptl2* signaling through PIR-B mediates this function. However, here we found that supplementation of recombinant ANGPTL2 protein activated expression of proinflammatory cytokines in GM-BMMs from *Pir-b* KO mice, an effect blocked in part by treatment with anti-integrin α5β1 antibodies. These findings show that ANGPTL2 mediates proinflammatory phenotypes in macrophages in part through the integrin α5β1 rather than the PIR-B receptor. One possibility is that an ANGPTL2/PIR-B pathway might serve a different function in GM-BMMs. In contrast, PIR-B is reportedly an inhibitory receptor, whereas the homologous PIR-A receptor is thought to be activating (33). Thus, ANGPTL2 might bind PIR-A. However, Zhang *et al.* (19) reported that ANGPTL2 does not bind to leukocyte immunoglobulin-like receptor A, an orthologue of mouse PIR-A. Fur-

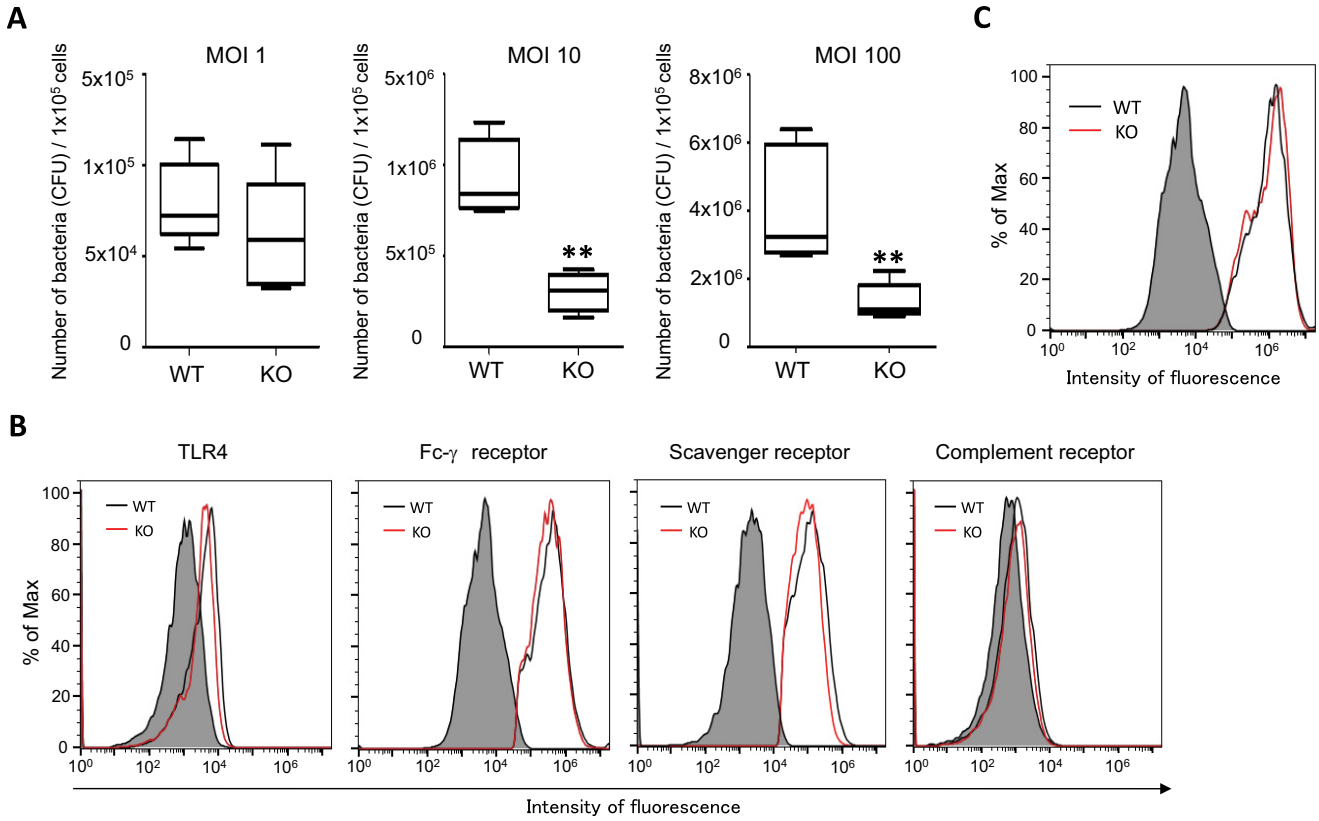

FIGURE 5. **Phagocytotic activity of GM-BMMs from WT and *Angptl2* KO mice.** *A*, phagocytotic activity of GM-BMMs from WT and *Angptl2* KO mice infected with LT2 at the indicated m.o.i. The number of intracellular bacteria was determined by cfu plate counts ($n = 10$). *B*, representative image showing FACS analysis of expression of various receptors associated with phagocytosis in GM-BMMs from WT and *Angptl2* KO mice. *Gray area*, isotype control antibody; *black line*, WT mice; *red line*, *Angptl2* KO mice. *C*, representative image showing FACS quantification of phagocytosis of latex bead-IgG complexes by GM-BMMs from WT and *Angptl2* KO mice. *Gray area*, negative control; *black line*, WT mice; *red line*, *Angptl2* KO mice. **, $p < 0.01$. Data are expressed as means ± S.E. (*error bars*) from one (*A*) or four (*B* and *C*) different experiments.

ther studies are needed to clarify ANGPTL2/PIR-A or -PIR-B signaling in this context.

We also show here that expression of receptors associated with phagocytosis such as TLR4, Fc-γ receptor, scavenger receptor, and complement receptor was comparable in GM-BMMs derived from WT and *Angptl2* KO mice. Conversely, *Angptl2* KO GM-BMMs show impaired phagocytosis of bacteria at higher m.o.i. values (>10). Phagocytosis is triggered by pattern recognition receptors and is accompanied by actin polymerization and activation of the GTPases Rac1, Rac2, and Cdc42 to enable formation of the phagocytic cup (34). We reported previously that ANGPTL2 activates the integrin α5β1/Rac pathway (11). Thus, ANGPTL2 may promote phagocytosis by activating actin polymerization through that pathway.

In addition to phagocytosis, activated macrophages also function to combat infection caused by intracellular pathogens. NO is a critical effector of macrophages in antipathogenic responses, and NO harbors direct antimicrobial activity (35–37). Here, using nitrite levels as a readout, we found that NO production by *Angptl2*-deficient macrophages in response to LT2 infection was lower than that seen in WT macrophages. We conducted a preliminary analysis to adoptively transfer WT macrophages into the peritoneum of LT2-infected *Angptl2* KO mice and observed that transfer tended to rescue survival (data not shown). These studies suggest that intracellular bacterial clearance, rather than phagocytosis, is impaired in *Angptl2* KO macrophages, but these conclusions require confirmation in future studies.

IL-1β family factors such as IL-1β and IL-33 induce NO in macrophages (38). Given that macrophages from *Angptl2* KO mice show attenuated expression of proinflammatory cytokines, including IL-1β, we conclude that this decrease underlies reduced NO production seen in macrophages from mutant mice. In addition, IFN-γ activates macrophages and promotes expression of antimicrobial effectors, including NO (39).

Proinflammatory polarization of macrophages requires Th1 cytokines, particularly T cell-derived IFN-γ (40). At day 3 after LT2 infection *in vivo*, we observed lower levels of serum IFN-γ in *Angptl2* KO compared with WT mice (data not shown). As our primary focus here is on macrophage function, we did not evaluate T cells in detail for this study. However, levels of IFN-γ produced by T cells may be reduced in *Angptl2* KO relative to WT mice, a possibility to be addressed in future studies.

In summary, we report that ANGPTL2 is predominantly expressed in proinflammatory macrophages and that macrophage-derived ANGPTL2 promotes proinflammatory phenotypes in part through the integrin α5β1 receptor. *Angptl2* KO mice are likely susceptible to infection due to attenuated NO production by *Angptl2*-deficient macrophages. These findings suggest an important role for ANGPTL2 in NO production by macrophages; however, further studies are necessary to deter-

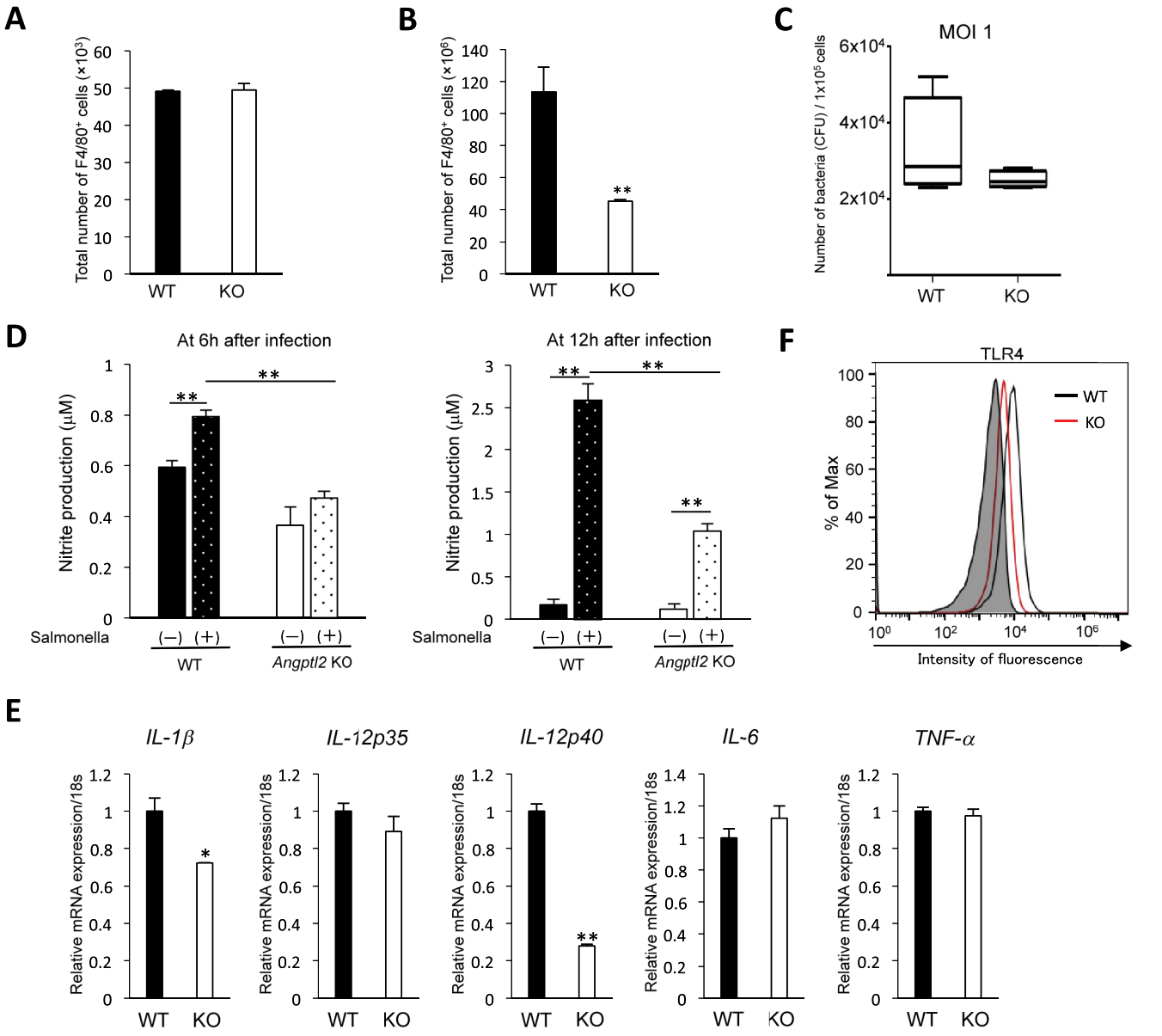

FIGURE 6. **Analysis of inflammatory phenotypes in peritoneal macrophages from WT and *Angptl2* KO mice.** *A*, the total number of peritoneal macrophages from WT and *Angptl2* KO mice in the unstimulated state ($n = 4$). *B*, comparable analysis 4 days after peritoneal injection of thioglycollate broth ($n = 4$). *C*, phagocytotic activity of macrophages from WT and *Angptl2* KO mice infected with LT2 at an m.o.i. of 1. The number of intracellular bacteria was determined by cfu plate counts ($n = 10$). *D*, NO production by peritoneal macrophages from WT and *Angptl2* KO mice infected with live LT2 at an m.o.i. of 1 at 6 (*left panel*) or 12 (*right panel*) h after infection with live LT2 as assessed by nitrite levels ($n = 4$). *E*, relative expression of mRNAs encoding proinflammatory markers in cultured peritoneal macrophages from WT and *Angptl2* KO mice stimulated with LPS ($n = 4$). Levels in WT were set at 1. *F*, representative image of FACS analysis to assess TLR4 expression in peritoneal macrophages from WT and *Angptl2* KO mice. *Gray area*, isotype control antibody; *black line*, WT; *red line*, *Angptl2* KO. *, $p < 0.05$; **, $p < 0.01$. Data are expressed as means ± S.E. (*error bars*) from one (*C*), two (*A*, *B*, *D*, and *E*), or four (*F*) different experiments.

mine whether ANGPTL2 directly increases NO production in these cells.

Experimental Procedures

Mice—Female *Angptl2*-deficient (*Angptl2* KO) and WT littermate mice on a C57BL/6N background were used for all experiments as described (11). *Pir-b*-deficient (*Pir-b* KO) mice were obtained from Dr. Takai (41). All procedures were approved by the Kumamoto University Ethics Review Committee for Animal Experimentation.

Culture of Bone Marrow Cells—Bone marrow-derived macrophages grown in M-CSF (eBioscience, San Diego, CA) or GM-CSF (PeproTech, Rocky Hill, NJ) were generated as described (42). Briefly, bone marrow cells were obtained from mouse femurs. After lysing erythrocytes, cells were cultured at 1×10^6 cells/ml in RPMI 1640 medium containing 10% FCS and 50 ng/ml M-CSF or 20 ng/ml GM-CSF conditioned medium for 2 days. After removing nonadherent cells, adherent cells were cultured in fresh medium for 4 more days and harvested for use as M-BMMs in the case of M-CSF-treated cells or GM-BMMs in the case of GM-CSF-treated cells.

Collection of Peritoneal Macrophages—After euthanizing mice, the outer skin of the peritoneum was cut, 5 ml of ice-cold phosphate-buffered saline (PBS) (with 3% FCS) was injected

into the peritoneal cavity, the peritoneum was gently massaged, and the perfusate was collected. The perfusate was then centrifuged at 2000 rpm for 5 min, and the supernatant was discarded. Precipitated cells were resuspended in RPMI 1640 medium containing 10% FCS. For induction analysis, mice were administered 4% thioglycollate (BD Biosciences) intraperitoneally. Resultant peritoneal exudate cells were collected at 4 days after treatment by 4% thioglycollate (43).

Quantitative Real Time PCR—Total RNA from M-BMMs or GM-BMMs was extracted using TRIzol reagent (Invitrogen), treated with DNase, and reverse transcribed with a PrimeScript RT reagent kit (Takara, Shiga, Japan). PCRs were performed using SYBR Premix Ex TaqII (Takara). Specific primer pairs are as follows: Angptl2: forward, 5′-GGAGGTTGGACTGTCATCCAGAG-3′; reverse, 5′-GCCTTGGTTCGTCAGCCAGTA-3′; IL-1β: forward, 5′-TCCAGGATGAGGACATGAGCAC-3′; reverse, 5′-GAACGTCACACACCAGCAGGTTA-3′; IL-6: forward, 5′-CCACTTCACAAGTCGGAGGCTTA-3′; reverse, 5′-GCAAGTGCATCATCGTTGTTCATAC-3′; IL-12p35: forward, 5′-TACTAGAGAGACTTCTTCCACAACAAGAG-3′; reverse, 5′-TCTGGTACATCTTCAAGTCCTCATAGA-3′; IL-12p40: forward, 5′-GACCATCACTGTCAAAGAGTTTCTAGAT-3′; reverse, 5′-AGGAAAGTCTTGTTTTTGAAATTTTTTAA-3′; TNF-α: forward, 5′-AAGCCTGTAGCCCACGTCGTA-3′; reverse, 5′-GGCACCACTAGTTGGTTGTCTTTG-3′; IL-10: forward, 5′-GCTCTTACTGACTGGCATGAG-3′; reverse, 5′-CGCAGCTCTAGGAGCATGTG-3′; CX3CR1: forward, 5′-AGTCTGCGTGAGACTGGGTGA-3′; reverse, 5′-AGATGGTTCCAAAGGCCACAA-3′; Rps18: forward, 5′-TTCTGGCCAACGGTCTAGACAAC-3′; reverse, 5′-CCAGTGGTCTTGGTGTGCTGA-3′. PCR products were analyzed using a Thermal Cycler Dice Real Time system (Takara), and relative transcript abundance was normalized to that of *Rps18* mRNA.

rANGPTL2 Treatment—Recombinant mouse ANGPTL2 hexahistidine-tagged protein was expressed in *Escherichia coli* Rosetta^{TM}pLacI cells (Merck) in inclusion bodies. Briefly, the bacterial cultures were grown in LB medium at 37 °C to midlog phase, and the protein was induced with isopropyl 1-thio-β-D-galactopyranoside at 13 °C for 18 h. The harvested cells (6 g) were suspended in 30 ml of ice-cold buffer (20 mM Hepes-NaOH, pH 7.4, 0.5 M NaCl, 0.05% Triton X-100, 1 mM PMSF) and thoroughly disrupted by sonication. The inclusion bodies were solubilized, reduced, and modified by 3-trimethylammoniopropyl methanethiosulfonate bromide (Wako, Osaka, Japan) according to a published procedure (44) with minor modifications. 3-Trimethylammoniopropyl methanethiosulfonate bromide-modified proteins were desalted on a Sephadex G-25 column (GE Healthcare). Desalted proteins were loaded onto a Talon column (Takara) and eluted with 0.15 M imidazole after washing the column with solubilizing buffer. The eluted sample was desalted again, and a portion of the sample was diluted into refolding buffer (2 μg/ml final concentration) containing 2 mM cysteine and 0.5 mM cystine at 4 °C for 14 h. Proteins were adsorbed onto a Source 30 reverse-phase matrix (GE Healthcare) and eluted with acetonitrile containing 0.04% trifluoroacetic acid. The eluate was freeze-dried, dissolved in 0.1% acetic acid, and stored at −80 °C. The samples had an endotoxin level less than 0.3 endotoxin unit/mg. GM-BMMs from *Angptl2* or *Pir-b* KO mice were plated at 2×10^5 cells/well in RPMI 1640 medium containing 10% FCS plus 20 ng/ml GM-CSF conditioned medium. Medium was then changed to fresh medium containing 1 μg/ml rANGPTL2 protein, and cells were then cultured for more than 6 h before analysis of inflammatory cytokine gene expression by quantitative real time PCR.

Integrin Assay—GM-BMMs from *Angptl2* KO mice were plated at 2×10^5 cells/well in RPMI 1640 medium containing 10% FCS plus 20 ng/ml GM-CSF conditioned medium with or without anti-mouse integrin $\alpha5\beta1$ antibody (Merck Millipore, Darmstadt, Germany) for 30 min. Medium was then changed to fresh medium containing 1 μg/ml rANGPTL2 protein, and cells were then cultured for 6 h before analysis of inflammatory cytokine gene expression by quantitative real time PCR.

Cell Adhesion Assay—Various concentrations of ANGPTL2 protein were coated onto 96-well flat bottomed plates overnight at 4 °C and blocked with 3% BSA for 1 h at 37 °C. GM-BMMs from WT mice were adjusted to 1×10^5cells/ml and preincubated in serum-free medium with or without anti-$\alpha5\beta1$ (Merck Millipore) for 30 min at 37 °C. Pretreated cells were incubated in the ANGPTL2 protein-coated dishes at 37 °C for 1 h. Non-adherent cells were removed by gentle PBS washing, and then adherent cells were fixed with 4% paraformaldehyde in PBS for 30 min and stained with 0.5% crystal violet in 25% methanol for 30 min. Plates were rinsed with tap water, stained cells were solubilized in 1% SDS, and the A_{595} value was determined.

Salmonella Infection—Mice were administered *Salmonella enterica* serovar Typhimurium LT2 in 0.1 ml of PBS intraperitoneally (i.p.). At various time points thereafter, body weights and mouse survival were monitored, and mice were sacrificed to obtain liver, spleen, and blood samples to assess bacterial growth. Organs were drawn into a heparin-coated tube and weighed. Liver and spleen were homogenized in 0.1% deoxycholic acid in PBS, and homogenates were serially diluted and subjected to a cfu assay on LB agar plates.

Quantitation of ANGPTL2 Protein—Plasma ANGPTL2 protein was quantified by ELISA. ANGPTL2 concentration was estimated using an ANGPTL2 Assay kit (Immuno-Biological Laboratories, Gunma, Japan) according to the manufacturer's instructions.

Nitrite Production Assay—GM-BMMs or peritoneal macrophages (1×10^5 cells) were plated onto 96-well plates in DMEM containing 10% FCS and stimulated with LT2 at an m.o.i. of 1. Cells were then incubated at 37 °C for various time periods under 5% CO_2 before supernatants were collected. Accumulation of nitrite, a stable metabolite of NO, in supernatants was quantified by a Griess reaction as described (29, 30). Briefly, 50-μl aliquots of culture supernatants were dispensed in triplicate into 96-well plates and mixed with 25 μl of Griess reagent A (1% sulfanilamide in 5% H_3PO_4). After incubation for 5 min, 25 μl of Griess reagent B (0.1% *N*-(1-naphthyl)-ethylenediamine) was added and incubated for 10 min at room temperature. Sample absorbance at 540 nm was compared with that of a sodium nitrite standard using a microplate reader (Bio-Rad).

Bacterial Phagocytosis Assay—For *in vitro* infection, LT2 (see above) was added at the indicated m.o.i. into 96-well plates containing GM-BMMs or peritoneal macrophages (1×10^5 cells/well). Cultures were centrifuged briefly and then incubated at 37 °C for 20 min under 5% CO_2 before addition of gentamicin (Wako) at a final concentration of 100 μg/ml for 30 min to kill extracellular LT2. After three PBS washes, infected cells were lysed in 0.1% deoxycholic acid in PBS before cfu plate counts were undertaken (45).

Flow Cytometry—A total of 5×10^5 GM-BMMs or peritoneal macrophages from WT or *Angptl2* KO mice were pretreated with 100-fold diluted Fc blocker (Fc-γ receptor) (CD16/32) (Bio Legend, San Diego, CA) for 15 min on ice. Cells were incubated with 100-fold diluted APC-anti-F4/80 (Bio Legend), 100-fold diluted APC-anti-CD284 (TLR4) (Bio Legend), 100-fold diluted phycoerythrin-anti-CD36 (scavenger receptor) (Bio Legend), 100-fold diluted APC-anti-CD21/CD35 (complement receptor) (Bio Legend), 100-fold diluted Alexa Fluor® 488 (Thermo Fisher Scientific Inc.) or the respective isotype-matched control IgG for 30 min at 4 °C and washed twice with PBS. To analyze macrophages only, we first confirmed areas harboring F4/80-positive cells and analyzed other antibody-positive cells by BD Accuri C6 flow cytometry (BD Biosciences) using FlowJo software (Treestar, Ashland, OR).

Bead Phagocytosis Assay—GM-BMMs from WT or *Angptl2* KO mice were plated onto 24-well plates at 5×10^5 cells/well in RPMI 1640 medium containing 10% FCS and incubated overnight at 37 °C. The next day, bead phagocytosis was quantified using a phagocytosis assay kit (Cayman, Ann Arbor, MI) according to the manufacturer's instructions. All samples were analyzed by BD Accuri C6 flow cytometry after samples were treated with assay buffer and vortexed (46).

Peritoneal Macrophage Cell Counts—Peritoneal macrophages from WT or *Angptl2* KO mice were pretreated with Fc blocker (Bio Legend) and incubated with APC-anti-F4/80 (Bio Legend). After incubation, counting beads (CountBright absolute counting beads, Invitrogen) were added as a reference to calculate absolute cell numbers. Cells were analyzed by BD Accuri C6 flow cytometry (47).

LPS Stimulation—Peritoneal macrophages from WT or *Angptl2* KO mice were plated at 2×10^5 cells/well in RPMI 1640 medium containing 10% FCS. Cells were cultured with or without 10 μg/ml LPS (Sigma) for 6 h before analysis of gene expression by quantitative real time PCR.

Statistical Analysis—Data were recorded as the mean ± S.E. Differences in group survival were analyzed using Mantel-Cox log rank p test. All other simple comparisons were performed using Student's t test with $p < 0.05$ considered statistically significant.

Author Contributions—M. Y., H. O., and M. E. designed the study and wrote the paper. M. Y., H. O., H. Tsutsuki, and S. F. performed *S. enterica* serovar Typhimurium experiments. M. Y., H. O., T. K., T. M., K. M., K. T., H. Tanoue, H. I., J. M., H. H., and T. Sugizaki performed *in vitro* and *in vivo* experiments and provided technical assistance. T. A., T. G., T. T., T. Sawa, H. M., and Y. O. provided supervision for conception of the study. All authors analyzed the results and approved the final version of the manuscript.

Acknowledgments—We thank K. Tabu, M. Nakata, and N. Shirai for technical assistance.

References

1. Akira, S., Uematsu, S., and Takeuchi, O. (2006) Pathogen recognition and innate immunity. *Cell* **124,** 783–801
2. Fritz, J. H., Ferrero, R. L., Philpott, D. J., and Girardin, S. E. (2006) Nod-like proteins in immunity, inflammation and disease. *Nat. Immunol.* **7,** 1250–1257
3. Pfeffer, K., Matsuyama, T., Kündig, T. M., Wakeham, A., Kishihara, K., Shahinian, A., Wiegmann, K., Ohashi, P. S., Krönke, M., and Mak, T. W. (1993) Mice deficient for the 55 kd tumor necrosis factor receptor are resistant to endotoxic shock, yet succumb to *L. monocytogenes* infection. *Cell* **73,** 457–467
4. Jouanguy, E., Döffinger, R., Dupuis, S., Pallier, A., Altare, F., and Casanova, J. L. (1999) IL-12 and IFN-γ in host defense against mycobacteria and salmonella in mice and men. *Curr. Opin. Immunol.* **11,** 346–351
5. Ehrt, S., Schnappinger, D., Bekiranov, S., Drenkow, J., Shi, S., Gingeras, T. R., Gaasterland, T., Schoolnik, G., and Nathan, C. (2001) Reprogramming of the macrophage transcriptome in response to interferon-γ and *Mycobacterium tuberculosis*: signaling roles of nitric oxide synthase-2 and phagocyte oxidase. *J. Exp. Med.* **194,** 1123–1140
6. Chacón-Salinas, R., Serafín-López, J., Ramos-Payán, R., Méndez-Aragón, P., Hernández-Pando, R., Van Soolingen, D., Flores-Romo, L., Estrada-Parra, S., and Estrada-García, I. (2005) Differential pattern of cytokine expression by macrophages infected in vitro with different *Mycobacterium tuberculosis* genotypes. *Clin. Exp. Immunol.* **140,** 443–449
7. Kiszewski, A. E., Becerril, E., Aguilar, L. D., Kader, I. T., Myers, W., Portaels, F., and Hernández Pando, R. (2006) The local immune response in ulcerative lesions of Buruli disease. *Clin. Exp. Immunol.* **143,** 445–451
8. Murphy, J. T., Sommer, S., Kabara, E. A., Verman, N., Kuelbs, M. A., Saama, P., Halgren, R., and Coussens, P. M. (2006) Gene expression profiling of monocyte-derived macrophages following infection with *Mycobacterium avium* subspecies *avium* and *Mycobacterium avium* subspecies *paratuberculosis*. *Physiol. Genomics* **28,** 67–75
9. Rottenberg, M. E., Gigliotti-Rothfuchs, A., and Wigzell, H. (2002) The role of IFN-γ in the outcome of chlamydial infection. *Curr. Opin. Immunol.* **14,** 444–451
10. Igietseme, J. U., Perry, L. L., Ananaba, G. A., Uriri, I. M., Ojior, O. O., Kumar, S. N., and Caldwell, H. D. (1998) Chlamydial infection in inducible nitric oxide synthase knockout mice. *Infect. Immun.* **66,** 1282–1286
11. Tabata, M., Kadomatsu, T., Fukuhara, S., Miyata, K., Ito, Y., Endo, M., Urano, T., Zhu, H. J., Tsukano, H., Tazume, H., Kaikita, K., Miyashita, K., Iwawaki, T., Shimabukuro, M., Sakaguchi, K., *et al.* (2009) Angiopoietin-like protein 2 promotes chronic adipose tissue inflammation and obesity-related systemic insulin resistance. *Cell Metab.* **10,** 178–188
12. Kubota, Y., Oike, Y., Satoh, S., Tabata, Y., Niikura, Y., Morisada, T., Akao, M., Urano, T., Ito, Y., Miyamoto, T., Watanabe, S., and Suda, T. (2005) Isolation and expression patterns of genes for three angiopoietin-like proteins, *Angptl1*, *2* and *6* in zebrafish. *Gene. Expr. Patterns* **5,** 679–685
13. Okada, T., Tsukano, H., Endo, M., Tabata, M., Miyata, K., Kadomatsu, T., Miyashita, K., Semba, K., Nakamura, E., Tsukano, M., Mizuta, H., and Oike, Y. (2010) Synoviocyte-derived angiopoietin-like protein 2 contributes to synovial chronic inflammation in rheumatoid arthritis. *Am. J. Pathol.* **176,** 2309–2319
14. Horio, E., Kadomatsu, T., Miyata, K., Arai, Y., Hosokawa, K., Doi, Y., Ninomiya, T., Horiguchi, H., Endo, M., Tabata, M., Tazume, H., Tian, Z., Takahashi, O., Terada, K., Takeya, M., *et al.* (2014) Role of endothelial cell-derived angptl2 in vascular inflammation leading to endothelial dysfunction and atherosclerosis progression. *Arterioscler. Thromb. Vasc. Biol.* **34,** 790–800
15. Tazume, H., Miyata, K., Tian, Z., Endo, M., Horiguchi, H., Takahashi, O., Horio, E., Tsukano, H., Kadomatsu, T., Nakashima, Y., Kunitomo, R., Kaneko, Y., Moriyama, S., Sakaguchi, H., Okamoto, K., *et al.* (2012) Macrophage-derived angiopoietin-like protein 2 accelerates development of abdominal aortic aneurysm. *Arterioscler. Thromb. Vasc. Biol.* **32,** 1400–1409

16. Cunnick, J., Kaur, P., Cho, Y., Groffen, J., and Heisterkamp, N. (2006) Use of bone marrow-derived macrophages to model murine innate immune responses. *J. Immunol. Methods* **311,** 96–105
17. Fleetwood, A. J., Lawrence, T., Hamilton, J. A., and Cook, A. D. (2007) Granulocyte-macrophage colony-stimulating factor (CSF) and macrophage CSF-dependent macrophage phenotypes display differences in cytokine profiles and transcription factor activities: implications for CSF blockade in inflammation. *J. Immunol.* **178,** 5245–5252
18. Lacey, D. C., Achuthan, A., Fleetwood, A. J., Dinh, H., Roiniotis, J., Scholz, G. M., Chang, M. W., Beckman, S. K., Cook, A. D., and Hamilton, J. A. (2012) Defining GM-CSF- and macrophage-CSF-dependent macrophage responses by *in vitro* models. *J. Immunol.* **188,** 5752–5765
19. Zhang, C. C., Kaba, M., Ge, G., Xie, K., Tong, W., Hug, C., and Lodish, H. F. (2006) Angiopoietin-like proteins stimulate *ex vivo* expansion of hematopoietic stem cells. *Nat. Med.* **12,** 240–245
20. Dougan, G., John, V., Palmer, S., and Mastroeni, P. (2011) Immunity to salmonellosis. *Immunol. Rev.* **240,** 196–210
21. Torii, I., Oka, S., Hotomi, M., Benjamin, W. H., Jr., Takai, T., Kearney, J. F., Briles, D. E., and Kubagawa, H. (2008) PIR-B-deficient mice are susceptible to *Salmonella* infection. *J. Immunol.* **181,** 4229–4239
22. Biswas, S. K., and Mantovani, A. (2010) Macrophage plasticity and interaction with lymphocyte subsets: cancer as a paradigm. *Nat. Immunol.* **11,** 889–896
23. Thäle, C., and Kiderlen, A. F. (2005) Sources of interferon-γ (IFN-γ) in early immune response to *Listeria monocytogenes*. *Immunobiology* **210,** 673–683
24. Mantovani, A. (2008) From phagocyte diversity and activation to probiotics: back to Metchnikoff. *Eur. J. Immunol.* **38,** 3269–3273
25. Nathan, C. F., and Hibbs, J. B., Jr. (1991) Role of nitric oxide synthesis in macrophage antimicrobial activity. *Curr. Opin. Immunol.* **3,** 65–70
26. Umezawa, K., Akaike, T., Fujii, S., Suga, M., Setoguchi, K., Ozawa, A., and Maeda, H. (1997) Induction of nitric oxide synthesis and xanthine oxidase and their roles in the antimicrobial mechanism against *Salmonella typhimurium* infection in mice. *Infect Immun.* **65,** 2932–2940
27. James, S. L. (1995) Role of nitric oxide in parasitic infections. *Microbiol. Rev.* **59,** 533–547
28. Alam, M. S., Akaike, T., Okamoto, S., Kubota, T., Yoshitake, J., Sawa, T., Miyamoto, Y., Tamura, F., and Maeda, H. (2002) Role of nitric oxide in host defense in murine salmonellosis as a function of its antibacterial and antiapoptotic activities. *Infect. Immun.* **70,** 3130–3142
29. Shimizu, T., Tsutsuki, H., Matsumoto, A., Nakaya, H., and Noda, M. (2012) The nitric oxide reductase of enterohaemorrhagic *Escherichia coli* plays an important role for the survival within macrophages. *Mol. Microbiol.* **85,** 492–512
30. Tsutsuki, H., Yahiro, K., Suzuki, K., Suto, A., Ogura, K., Nagasawa, S., Ihara, H., Shimizu, T., Nakajima, H., Moss, J., and Noda, M. (2012) Subtilase cytotoxin enhances *Escherichia coli* survival in macrophages by suppression of nitric oxide production through the inhibition of NF-κB activation. *Infect Immun.* **80,** 3939–3951
31. Kadomatsu, T., Endo, M., Miyata, K., and Oike, Y. (2014) Diverse roles of ANGPTL2 in physiology and pathophysiology. *Trends Endocrinol. Metab.* **25,** 245–254
32. Martin, A. M., Kulski, J. K., Witt, C., Pontarotti, P., and Christiansen, F. T. (2002) Leukocyte Ig-like receptor complex (LRC) in mice and men. *Trends Immunol.* **23,** 81–88
33. Ravetch, J. V., and Lanier, L. L. (2000) Immune inhibitory receptors. *Science* **290,** 84–89
34. Weiss, G., and Schaible, U. (2015) Macrophage defense mechanisms against intracellular bacteria. *Immunol. Rev.* **264,** 182–203
35. Henard, C. A., and Vázquez-Torres, A. (2011) Nitric oxide and salmonella pathogenesis. *Front. Microbiol.* **2,** 84
36. Wink, D. A., Hines, H. B., Cheng, R. Y., Switzer, C. H., Flores-Santana, W., Vitek, M. P., Ridnour, L. A., and Colton, C. A. (2011) Nitric oxide and redox mechanisms in the immune response. *J. Leukoc. Biol.* **89,** 873–891
37. Nathan, C., and Shiloh, M. (2000) Reactive oxygen and nitrogen intermediates in the relationship between mammalian hosts and microbial pathogens. *Proc. Natl. Acad. Sci. U.S.A.* **97,** 8841–8848
38. Lima-Junior, D. S., Costa, D. L., Carregaro, V., Cunha, L. D., Silva, A. L., Mineo, T. W., Gutierrez, F. R., Bellio, M., Bortoluci, K. R., Flavell, R. A., Bozza, M. T., Silva, J. S., and Zamboni, D. S. (2013) Inflammasome-derived IL-1β production induces nitric oxide-mediated resistance to *Leishmania*. *Nat. Med.* **19,** 909–915
39. Bogdan, C. (2001) Nitric oxide and the immune response. *Nat. Immunol.* **2,** 907–916
40. Bogdan, C. (2015) Nitric oxide synthase in innate and adaptive immunity: an update. *Trends Immunol.* **36,** 161–178
41. Ujike, A., Takeda, K., Nakamura, A., Ebihara, S., Akiyama, K., and Takai, T. (2002) Impaired dendritic cell maturation and increased T_H2 responses in PIR-B(−/−) mice. *Nat. Immunol.* **3,** 542–548
42. Lari, R., Fleetwood, A. J., Kitchener, P. D., Cook, A. D., Pavasovic, D., Hertzog, P. J., and Hamilton, J. A. (2007) Macrophage lineage phenotypes and osteoclastogenesis—complexity in the control by GM-CSF and TGF-β. *Bone* **40,** 323–336
43. Melnicoff, M. J., Horan, P. K., Breslin, E. W., and Morahan, P. S. (1988) Maintenance of peritoneal macrophages in the steady state. *J. Leukoc. Biol.* **44,** 367–375
44. Terzyan, S. S., Peracaula, R., de Llorens, R., Tsushima, Y., Yamada, H., Seno, M., Gomis-Rüth, F. X., and Coll, M. (1999) The three-dimensional structure of human RNase 4, unliganded and complexed with d(Up), reveals the basis for its uridine selectivity. *J. Mol. Biol.* **285,** 205–214
45. Chakravortty, D., Hansen-Wester, I., and Hensel, M. (2002) *Salmonella* pathogenicity island 2 mediates protection of intracellular *Salmonella* from reactive nitrogen intermediates. *J. Exp. Med.* **195,** 1155–1166
46. Beletskii, A., Cooper, M., Sriraman, P., Chiriac, C., Zhao, L., Abbot, S., and Yu, L. (2005) High-throughput phagocytosis assay utilizing a pH-sensitive fluorescent dye. *BioTechniques* **39,** 894–897
47. Haverslag, R. T., de Groot, D., Grundmann, S., Meder, B., Goumans, M. J., Pasterkamp, G., Hoefer, I. E., and de Kleijn, D. P. (2013) CD26 inhibition enhances perfusion recovery in ApoE−/− mice. *Curr. Vasc. Pharmacol.* **11,** 21–28